The 1D spin-$\frac{1}{2}$ AF-Heisenberg model in a staggered field[*]

A. Fledderjohann, M. Karbach[a], and K.-H. Mütter

Physics Department, University of Wuppertal, 42097 Wuppertal, Germany

Abstract. We investigate the scaling properties of the excitation energies and transition amplitudes of the one-dimensional spin-$\frac{1}{2}$ antiferromagnetic Heisenberg model exposed to an external perturbation. Two types of perturbations are discussed in detail: a staggered field and a dimerized field.

PACS. 75.10.-b General theory and models of magnetic ordering

1 Introduction

The one-dimensional spin-$\frac{1}{2}$ antiferromagnetic Heisenberg model with nearest neighbour couplings and periodic boundary conditions ($\mathbf{S}_{N+1} = \mathbf{S}_1$):

$$\mathbf{H} \equiv 2\sum_{l=1}^{N} \mathbf{S}_l \cdot \mathbf{S}_{l+1} \qquad (1.1)$$

has been studied intensively with analytic and numerical methods. Eigenvalues as well as transition matrix elements for the spin operator have been calculated with the Bethe ansatz and quantum group symmetries [1]. These calculations allow to exploit part of the dynamical properties of the model, the two-spinon contributions, at $T = 0$ [2]. The dynamics of the model in the presence of an external magnetic field, which is periodic in space

$$\mathbf{H}(h) \equiv \mathbf{H} + h\mathbf{S}_3(q) \qquad (1.2)$$

with

$$\mathbf{S}_3(q) \equiv \sum_{l=1}^{N} e^{ilq} S_l^3, \qquad (1.3)$$

has been studied so far mainly for $q = 0$ [3–9]. Since the total spin $\mathbf{S}_3(0)$ commutes with $\mathbf{H}$, the eigenvectors of $\mathbf{H}(h)$ and $\mathbf{H}$ are the same, the eigenvalues change in a trivial manner. For this reason the magnetic properties of the model (1.1) in a constant field – as there are magnetization curves, susceptibilities, static and dynamic structure factors – were accessible by means of the Bethe ansatz as well. The case of a staggered field, *i.e.* equation (1.2) for $q = \pi$, in a one-dimensional Heisenberg model has attracted considerable interest as an effective model for

coupled spin chains. Treating the interchain coupling in the mean field approach, reduces the system to a one-dimensional Heisenberg model in a staggered field [10].

It is the purpose of this paper to study excitation energies

$$\omega_{mn}(N, h) \equiv E_m(N, h) - E_n(N, h), \qquad (1.4)$$

and transition amplitudes

$$T_{mn}(N, h) \equiv \langle \Psi_m(h)|\mathbf{S}_3(\pi)|\Psi_n(h)\rangle, \qquad (1.5)$$

for the operator $\mathbf{S}_3(\pi)$ in the one-dimensional antiferromagnetic Heisenberg model in a staggered field of strength h.

In Section 2 we derive a system of differential equations, which describes the evolution in h for ω_{mn} and T_{mn}. Section 3 is devoted to a finite-size scaling analysis of the ground state excitations ω_{m0} and T_{m0} in the combined limit $h \to 0$ and $N \to \infty$. It is shown in Section 4, that the critical exponents σ and ϵ in the scaling ansatz and the scaling variable as well can be computed by means of the evolution equations. For small values of the scaling variable the scaling function is also determined. In Section 5 we analyse in the same way the dimer operator.

2 Evolution equation for excitation energies and transition amplitudes

Starting from the eigenvalue equation of the Hamiltonian (1.2)

$$\mathbf{H}(h)|\Psi_n(h)\rangle = E_n(N, h)|\Psi_n(h)\rangle, \qquad (2.1)$$

it is straightforward to derive the evolution equations for the energy eigenvalues and eigenstates:

$$\frac{dE_n(N, h)}{dh} = T_{nn}(N, h), \qquad (2.2)$$

$$\frac{d}{dh}|\Psi_n(h)\rangle = -\sum_{m \neq n} \frac{T_{mn}(N, h)}{\omega_{mn}(N, h)}|\Psi_m(h)\rangle, \qquad (2.3)$$

---

[*] Dedicated to J. Zittartz on the occasion of his 60th birthday
[a] e-mail: `karbach@wptsb.uni-wuppertal.de`

where we have used the definitions (1.4) and (1.5).

The evolution is governed by the transition matrix elements of the operator $\mathbf{S}_3(\pi)$ (Eq. (1.3)). The operator $\mathbf{S}_3(\pi)$ is real hermitian and therefore the matrix (1.5) is symmetric $T_{mn} = T_{nm}$.

Remarkably enough, there exists a closed system of differential equations, which describes the h-dependence of the energy eigenvalues $E_n = E_n(N, h)$ and the transition matrix elements $T_{mn} = T_{mn}(N, h)$:

$$\frac{d^2 E_n}{dh^2} = -2 \sum_{l \neq n} \frac{|T_{ln}|^2}{\omega_{ln}}, \tag{2.4}$$

$$\frac{dT_{mn}}{dh} = -\sum_{l \neq m,n} \left[\frac{T_{ml} T_{ln}}{\omega_{lm}} + \frac{T_{ml} T_{ln}}{\omega_{ln}} \right] - \frac{T_{mn}}{\omega_{nm}} \frac{d\omega_{nm}}{dh} . \tag{2.5}$$

The Hamiltonian (1.2) behaves under translations $\mathbf{T}$ of one lattice spacing as:

$$\mathbf{T}\mathbf{H}(h)\mathbf{T}^\dagger = \mathbf{H}(-h). \tag{2.6}$$

Since $\mathbf{T}$ is unitary, the eigenvalues

$$E_n(N, h) = E_n(N, -h) \tag{2.7}$$

are symmetric, whereas the eigenstates $|\Psi(h)\rangle$,

$$|\Psi(-h)\rangle = \mathbf{T}|\Psi(h)\rangle, \tag{2.8}$$

are no longer momentum eigenstates, but linear combinations of two momentum eigenstates with momenta $p = 0$ and $p = \pi$, respectively. Of course, in the limit $h \to 0$ translation invariance is recovered and p is again a good quantum number. We use the following notation for the energy eigenstates:

$$\mathbf{T}|\Psi_n(0)\rangle = \pm|\Psi_n(0)\rangle, \quad n = 0, 1, 2, \ldots, \tag{2.9}$$

which means these states carry momentum $p = 0$ or $p = \pi$, respectively. The ordering of the energy eigenstates is chosen in such a way that the ground state $|\Psi_0(0)\rangle$ belongs to the ordered sequence of eigenstates with $n = 0, 2, 4, \ldots$ All eigenstates in this series have the same momentum. The series of eigenstates with $n = 1, 3, 5, \ldots$ carries the opposite sign. It starts with the first excitation $|\Psi_1(0)\rangle$ and is independently ordered.

Since the operator $\mathbf{S}_3(\pi)$ changes the momentum of the state by π, we get immediately from momentum conservation:

$$T_{mn}(N, 0) = 0 \quad \text{for} \quad (-1)^{m+n} = 1. \tag{2.10}$$

The transition matrix elements $T_{m0}(N, 0), m = 1, 3, 5, \ldots$ from the ground state $|\Psi_0(0)\rangle$ to the excited states $|\Psi_m(0)\rangle$ appear in the definition of the dynamic structure factor

$$S(N, \omega, p = \pi, h = 0) =$$
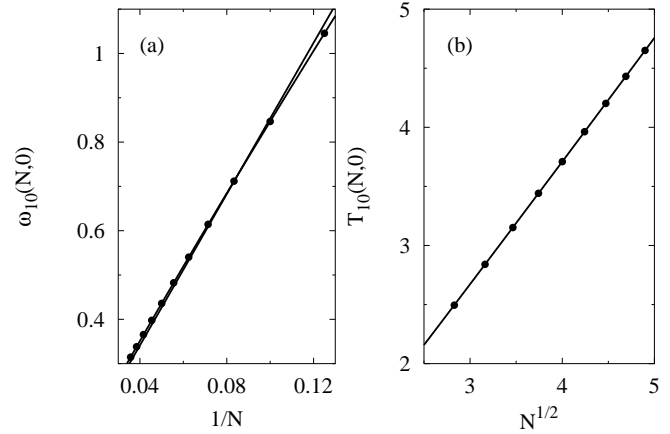$$\frac{1}{N} \sum_m \delta[\omega - \omega_{m0}(N, 0)]|T_{m0}(N, 0)|^2, \tag{2.11}$$

Fig. 1. Finite-size dependence of the ground state energy (a) and the corresponding transition amplitude (b) of Hamiltonian (1.2), for system sizes $N = 8, 10, \ldots, 24 \, (\bullet)$. The solid lines represent fits to the asymptotic behaviour (2.13) and (2.14).

which is known to develop an infrared singularity in the thermodynamic limit [2]:

$$S(\infty, \omega, \pi, 0) \stackrel{\omega \to 0}{\longrightarrow} A\frac{\sqrt{|\ln \omega|}}{\omega} . \tag{2.12}$$

The gap between the ground state and the excited states vanishes in the thermodynamic limit:

$$\omega_{m0}(N, 0) \stackrel{N \to \infty}{\longrightarrow} \frac{a_{m0}}{N} . \tag{2.13}$$

The coefficients a_{m0} can be computed in principle by the methods of conformal invariance and finite-size scaling [11–13]. The next order terms entering in equation (2.13) are logarithmic corrections. For this reason it becomes difficult to fix these coefficients from our system sizes up to $N = 24$. The difficulty of this task is extensively discussed in references [12,14–18]. In Figure 1a, a fit without logarithmic corrections ($a_{10} = 8.53$) and with logarithmic corrections ($a_{10} = 9.74$) is shown. The exact value is $a_{10} = \pi^2 = 9.86 \ldots$ [13].

Neglecting the logarithmic corrections in the large-N behaviour, we expect for the transition amplitudes:

$$T_{m0}(N, 0) \stackrel{N \to \infty}{\longrightarrow} b_{m0} N^\kappa, \quad m = 1, 3, \ldots \tag{2.14}$$

The exponent κ turns out to be $\kappa \simeq 1/2$, as can be seen from the numerical data for $T_{10}(N, 0)$ in Figure 1b. This is in agreement with conformal field theory, from which in the present case follows $\kappa = a_{10}/2\pi^2$ (See [19,20] and references therein). We consider equations (2.10, 2.13, 2.14) as initial conditions for the system of differential equations (2.4, 2.5).
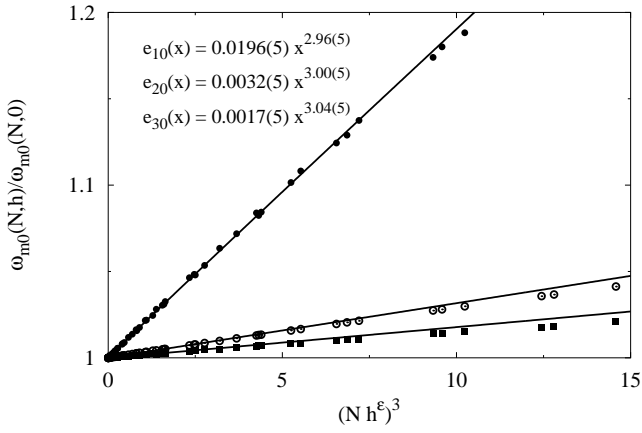
Fig. 2. The ratio (3.1) for $m = 1, 2, 3$ *versus* $(Nh^\epsilon)^3$ with $\epsilon = 0.66$. The solid lines show the fits to the small x-behaviour of $e_{m0}(x)$ (*cf.* (3.5)).
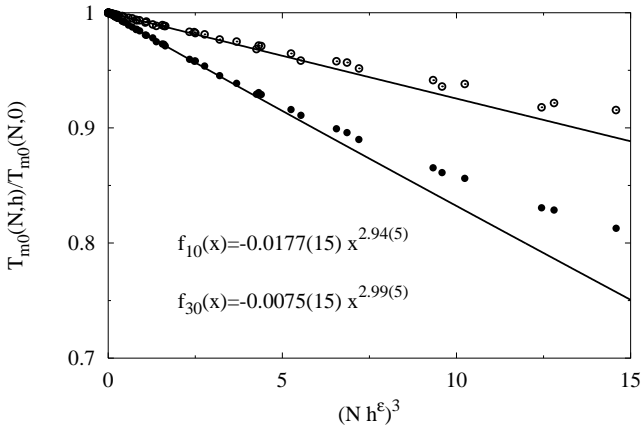

Fig. 3. The ratio (3.2) for $m = 1, 3$ *versus* $(Nh^\epsilon)^3$ with $\epsilon = 0.66$. The solid lines show the fits to the small x-behaviour of $f_{m0}(x)$ (*cf.* (3.6)).

3 The finite-size scaling analysis

In this section we present numerical evidence for the validity of a finite-size scaling ansatz:

$$\frac{\omega_{m0}(N,h)}{\omega_{m0}(N,0)} = 1 + e_{m0}(x), \qquad (3.1)$$

$$\frac{T_{m0}(N,h)}{T_{m0}(N,0)} = 1 + f_{m0}(x), \quad m = 1, 3, \ldots, \qquad (3.2)$$

in the combined limit

$$N \longrightarrow \infty, \quad h \longrightarrow 0, \quad \text{with fixed} \quad x \equiv Nh^\epsilon. \qquad (3.3)$$

Note, standard finite-size scaling theory [21,22] usually employ $y = x^{1/\epsilon}$ as the scaling variable. For our purpose it is more convenient to use x instead.

In Figures 2 and 3 we show our numerical results for the ratios (3.1, 3.2) on finite systems with $N = 8, 10, ..., 24$.
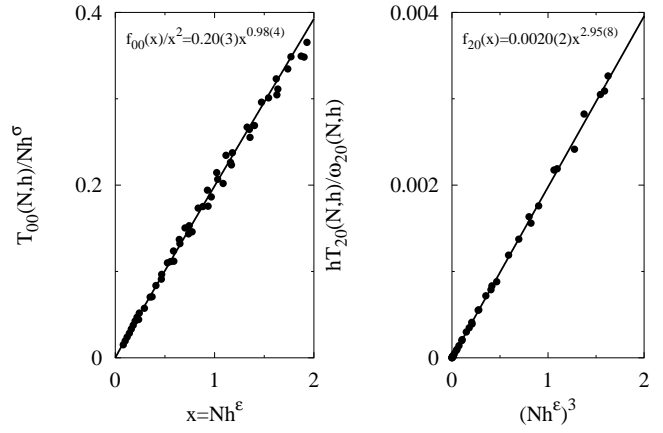

Fig. 4. The scaling behaviour of the transition amplitudes $T_{00}(N, h)$ and $T_{20}(N, h)$ for small x (see Eqs. (3.8, 3.10)).

The best results are achieved for

$$\epsilon = 0.66(1). \qquad (3.4)$$

The small x-behaviour of the scaling functions is well parametrised by:

$$e_{m0}(x) = e_{m0}x^{\phi_e}, \qquad (3.5)$$

$$f_{m0}(x) = f_{m0}x^{\phi_f}, \qquad (3.6)$$

with

$$\phi_e = \phi_f = 3.00(4). \qquad (3.7)$$

The diagonal matrix elements of the staggered operator $\mathbf{S}_3(\pi)$ vanish in the limit $h \to 0$ (*cf.* Eq. (2.10)). Therefore, a scaling ansatz of the type (3.2) does not make sense. However, according to (2.2) the diagonal matrix elements of $\mathbf{S}_3(\pi)$ can be identified with the first derivative of the corresponding energy eigenvalue. Assuming, that these scale in the same manner (3.1) as the excitation energies, we expect:

$$T_{00}(N,h) \to Nh^\sigma f_{00}(x)x^{-2}, \qquad (3.8)$$

with $\sigma = 1/3$. In Figure 4 we have plotted $T_{00}(h)/Nh^\sigma$ *versus* the scaling variable $x = Nh^\epsilon$. The scaling hypothesis works fairly well.

Moreover, the scaling function

$$f_{00}(x)x^{-2} \xrightarrow{x \to 0} f_{00}x, \qquad (3.9)$$

shows for small x-values a power behaviour, which is in agreement with (3.6) and (3.7). Finally, let us turn to the transition amplitude $T_{20}(h)$, which also vanishes in the limit $h \to 0$. In Figure 4 we have plotted

$$h\frac{T_{20}(N,h)}{\omega_{20}(N,h)} = f_{20}(x), \qquad (3.10)$$

versus the scaling variable x^3. Here we have assumed that T_{20} and ω_{20}/h scale in the same manner. This is indeed

the case as can be seen in Figure 4. Moreover, in the small x region the scaling function behaves as it is expected from (3.6) and (3.7).

In summary we observe that the excitation energies – with respect to the ground state – scale with h^ϵ ($\epsilon \simeq 2/3$):

$$\omega_{m0}(N,h) = h^\epsilon \Omega_{m0}(x). \qquad (3.11)$$

As before, we have neglected logarithmic corrections due to marginal operators. These corrections were deduced by means of conformal field theory [23]. The transition amplitudes scale with $h^\sigma N$ ($\sigma \simeq 1/3$):

$$T_{m0}(N,h) = N h^\sigma \Theta_{m0}(x). \qquad (3.12)$$

The small x-behaviour of the scaling functions $\Omega_{m0}(x)$ and $\Theta_{m0}(x)$ is fixed by the initial conditions (2.13, 2.14):

$$\Omega_{m0}(x) = a_{m0} x^{-1}[1 + e_{m0}(x)], \quad m = 0,1,2, \ldots \qquad (3.13)$$

According to (2.10) and (2.13) the small x-behaviour of different $\Theta_{m0}(x)$ is different for m even and m odd, respectively:

$$\Theta_{m0}(x) = \begin{cases} a_{m0} x^{-2} f_{m0}(x) & : (-1)^m = 1 \\ b_{m0} x^{-1/2}[1 + f_{m0}(x)] & : (-1)^m = -1. \end{cases} \qquad (3.14)$$

Again b_{m0} is given by the initial condition (2.14). The large x-behaviour of the scaling function for the first excitation is of special interest. If

$$\lim_{x \to \infty} \Omega_{10}(x) = \Omega_{10}^\infty \qquad (3.15)$$

is finite, equation (3.11) tells us that there is a gap in the thermodynamic limit, which opens with $h^\epsilon, \epsilon \simeq 2/3$. We have analysed our finite system data with the BST [24] algorithm and found:

$$\Omega_{10}^\infty = 4. \qquad (3.16)$$

A similar statement can be derived from equation (3.12) for the staggered magnetization, which can be expressed in terms of the transition matrix elements $T_{m0}(N,h)$:

$$m^\dagger(h) = \sum_m |T_{m0}(N,h)|^2. \qquad (3.17)$$

4 The evolution equation in the scaling limit

The critical exponents $\sigma = 1/3$ and $\epsilon = 2/3$ in equations (3.11, 3.12) as well as the small x-behaviour $\phi = 3$ of the scaling functions shown in Figures 2, 3 and 4 will now be derived from the evolution equations (2.2) and (2.3) in the scaling limit (3.3). We assume that a scaling ansatz of the type (3.11) and (3.12)

$$\omega_{mn}(N,h) = h^\epsilon \Omega_{mn}(x), \qquad (4.1)$$
$$T_{mn}(N,h) = N h^\sigma \Theta_{mn}(x), \qquad (4.2)$$

with the scaling variable

$$x = N h^\epsilon, \qquad (4.3)$$

holds for all the transition energies and amplitudes. Furthermore, let us assume that the small x-behaviour of the scaling functions:

$$\Omega_{mn}(x) \xrightarrow{x \to 0} a_{mn} x^{-1}[1 + e_{mn}(x)], \qquad (4.4)$$

$$\Theta_{mn}(x) \xrightarrow{x \to 0} \begin{cases} a_{mn} x^{-2} f_{mn}(x) & : (-1)^{n+m} = 1 \\ b_{mn} x^{-\sigma/\epsilon}[1 + f_{mn}(x)] & : (-1)^{n+m} = -1 \end{cases}, \qquad (4.5)$$

follows from the initial conditions:

$$\lim_{N \to \infty} N \omega_{mn}(N,0) = a_{mn}, \qquad (4.6)$$

and

$$T_{mn}(N,0) \xrightarrow{N \to \infty} b_{mn} N^\kappa \qquad (4.7)$$

where $b_{mn} = 0$ for $(-1)^{m+n} = +1$. The exponents κ, σ and ϵ are then related:

$$\kappa = 1 - \frac{\sigma}{\epsilon}. \qquad (4.8)$$

Now we discuss the evolution equations (2.4) and (2.5) in the scaling limit (3.3), in conjunction with the scaling ansatz (4.1, 4.2). It is convenient to inspect the derivative

$$D_1 = N^{-2} h^{-3\epsilon+2} \frac{d^2}{dh^2} \omega_{mn}(N,h). \qquad (4.9)$$

Then the left- and right-hand sides of (2.4) acquire the following form:

$$D_1 = \epsilon(\epsilon-1) x^{-2} \Omega_{mn}(x)$$
$$+ \epsilon(3\epsilon-1) x^{-1} \frac{d\Omega_{mn}(x)}{dx} + \epsilon^2 \frac{d^2 \Omega_{mn}(x)}{dx^2}, \qquad (4.10)$$

$$D_1 = 2 h^{2\sigma-4\epsilon+2}$$
$$\times \left[2 \frac{\Theta_{mn}^2(x)}{\Omega_{mn}(x)} - \sum_{l \neq m,n} \frac{\Theta_{lm}^2(x)}{\Omega_{lm}(x)} + \sum_{l \neq m,n} \frac{\Theta_{ln}^2(x)}{\Omega_{ln}(x)} \right]. \qquad (4.11)$$

A similar calculation for the derivative:

$$D_2 = h \frac{d}{dh} \ln [T_{mn}(N,h) \omega_{mn}(N,h)] \qquad (4.12)$$

yields for the left and right-hand sides of equation (2.5):

$$D_2 = (\sigma + \epsilon) + \epsilon x \frac{d}{dx} \ln[\Theta_{mn}(x) \Omega_{mn}(x)], \qquad (4.13)$$

$$D_2 = -h^{\sigma-2\epsilon+1} x$$
$$\times \sum_{l \neq m,n} \frac{\Theta_{ml}(x) \Theta_{ln}(x)}{\Theta_{mn}(x)} \left[\frac{1}{\Omega_{lm}(x)} + \frac{1}{\Omega_{ln}(x)} \right]. \qquad (4.14)$$

The corresponding left-hand sides and right-hand sides in (4.9) and (4.12) scale in the same manner provided that

$$\sigma = 2\epsilon - 1. \tag{4.15}$$

In this case (4.1) and (4.2) lead to a system of differential equations for the scaling functions $\Omega_{mn}(x)$ and $\Theta_{mn}(x)$.

Combining (4.15) and (4.8) we see that the exponents

$$\epsilon = \frac{1}{1+\kappa}, \quad \sigma = \frac{1-\kappa}{1+\kappa}, \tag{4.16}$$

are fixed by the exponent κ in the initial conditions (4.7).

The small x-behaviour is governed by the initial conditions (2.14) and (2.13). They tell us that the leading behaviour of the right-hand side of (4.11) arise from excitations with $(-1)^{l+m} = -1$ and $(-1)^{l+n} = -1$

$$\lim_{x \to 0} \frac{\Theta_{lm}^2(x)}{\Omega_{lm}(x)} = \frac{b_{lm}^2}{a_{lm}} x^{1-2\sigma/\epsilon}. \tag{4.17}$$

Therefore, the terms in (4.11) should be proportional to $x^{-3+2/\epsilon}$. Assuming that the small x-behaviour of functions $e_{mn}(x)$ can be described by a power law ansatz:

$$e_{mn}(x) = e_{mn} x^{\phi_e} + \dots, \tag{4.18}$$

it follows from (4.10) that

$$D_1 = a_{mn} e_{mn} x^{\phi_e - 3} \phi_e \epsilon (\phi_e \epsilon - 1) \tag{4.19}$$

is also proportional to $x^{-3+2/\epsilon}$ if

$$\phi_e = \frac{2}{\epsilon} . \tag{4.20}$$

Therefore, the first coefficient e_{mn} in the scaling function $e_{mn}(x)$ is completely fixed by the initial values a_{ln}, b_{lm}:

$$2e_{mn} = 2\left(1 - (-1)^{m+n}\right) \frac{b_{mn}^2}{a_{mn}^2}$$
$$- \frac{1}{a_{mn}} \sum_{l \neq m,n} \left[\left(1 - (-1)^{l+m}\right) \frac{b_{lm}^2}{a_{lm}} - \left(1 - (-1)^{l+n}\right) \frac{b_{ln}^2}{a_{ln}}\right]. \tag{4.21}$$

Next we study the small x-behaviour of (4.12). We will discuss the two cases $(-1)^{m+n} = 1$ and $(-1)^{m+n} = -1$ separately.

4.1 $(-1)^{m+n} = 1$

The right-hand side of (4.14) is governed by the excitations with $(-1)^{l+m} = -1$ and $(-1)^{l+n} = -1$:

$$x \frac{\Theta_{ml}(x)\Theta_{ln}(x)}{\Theta_{mn}(x)} \left[\frac{1}{\Omega_{lm}(x)} + \frac{1}{\Omega_{ln}(x)}\right]$$
$$\xrightarrow{x \to 0} \frac{b_{ml} b_{ln}}{a_{mn}} \left[\frac{1}{a_{lm}} + \frac{1}{a_{ln}}\right] \frac{x^{2/\epsilon}}{f_{mn}(x)}, \tag{4.22}$$

For the left-hand side of (4.13) we get:

$$3\epsilon - 1 + \epsilon x \frac{d}{dx} \ln[\Theta_{mn}(x)\Omega_{mn}(x)]$$
$$\xrightarrow{x \to 0} -1 + \epsilon x \frac{d}{dx} \ln f_{mn}(x). \tag{4.23}$$

Consistency of (4.22) and (4.23) is achieved if

$$f_{mn}(x) \xrightarrow{x \to 0} f_{mn} x^{\phi_f}, \tag{4.24}$$

with $\phi_f = \phi_e = 2/\epsilon$. The coefficient f_{mn} in (4.24) is completely fixed by the initial conditions:

$$f_{mn} = - \sum_{l \neq m,n} \frac{1 - (-1)^{l+m}}{2} \frac{1 - (-1)^{l+n}}{2}$$
$$\times \frac{b_{ml} b_{ln}}{a_{mn}} \left(\frac{1}{a_{lm}} + \frac{1}{a_{ln}}\right). \tag{4.25}$$

4.2 $(-1)^{m+n} = -1$

The contributions in (4.14) vanish:

$$x \frac{\Theta_{ml}(x)\Theta_{ln}(x)}{\Theta_{mn}(x)} \left[\frac{1}{\Omega_{lm}(x)} + \frac{1}{\Omega_{ln}(x)}\right]$$
$$\xrightarrow{x \to 0} \frac{1 + (-1)^{m+l}}{2} \frac{b_{ln} a_{ml}}{b_{mn}} \left[\frac{1}{a_{ln}} + \frac{1}{a_{lm}}\right] f_{ml}(x)$$
$$+ \frac{1 + (-1)^{n+l}}{2} \frac{b_{ml} a_{ln}}{b_{mn}} \left[\frac{1}{a_{ml}} + \frac{1}{a_{nl}}\right] f_{ln}(x), \tag{4.26}$$

since the scaling function f_{lm} vanishes for the excitations with $(-1)^{l+m} = 1$, according to equation (4.24). The leading behaviour of (4.13):

$$3\epsilon - 1 + \epsilon x \frac{d}{dx} \ln[\Theta_{mn}(x)\Omega_{mn}(x)]$$
$$\xrightarrow{x \to 0} \epsilon \left(\frac{d}{dx} f_{mn}(x) + e_{mn} x^{2/\epsilon}\right) \tag{4.27}$$

is governed by the scaling functions $e_{mn}(x)$ and $f_{mn}(x)$ for the excitations with $(-1)^{m+n} = -1$. Combining (4.26) and (4.27) we obtain:

$$2(e_{mn} + f_{mn})$$
$$= \sum_{l \neq m,n} \frac{1 + (-1)^{l+m}}{2} f_{ml} \frac{b_{ln} a_{ml}}{b_{mn}} \left[\frac{1}{a_{ml}} + \frac{1}{a_{ln}}\right]$$
$$+ \sum_{l \neq m,n} \frac{1 + (-1)^{l+n}}{2} f_{ln} \frac{b_{ml} a_{ln}}{b_{mn}} \left[\frac{1}{a_{ml}} + \frac{1}{a_{ln}}\right]. \tag{4.28}$$

In summary we conclude:

1. For consistency, all the scaling functions:

$$e_{mn}(x) = e_{mn} x^{\phi} + e_{mn}^{(1)} x^{\phi_1} + \dots, \tag{4.29}$$
$$f_{mn}(x) = f_{mn} x^{\phi} + f_{mn}^{(1)} x^{\phi_1} + \dots, \tag{4.30}$$

have the same small x-behaviour with exponent $\phi = 2/\epsilon$.

2. Equations (4.21), (4.25) and (4.28) enable us to express the first coefficients e_{mn}, f_{mn} in terms of the initial values a_{lm}, b_{lm}.

3. Having determined the lowest order in x of the scaling functions, we can proceed and compute the next order x^{ϕ_1} from the differential equations (4.9) and (4.12). The exponent ϕ_1 turns out to be $\phi_1 = 2\phi = 4/\epsilon$ for all the scaling functions. Moreover, the next order coefficients $e_{mn}^{(1)}, f_{mn}^{(1)}$ can be expressed again in terms of the initial values a_{mn}, b_{mn} and the zeroth order coefficients e_{mn}, f_{mn}.

4. The power ansatz ansatz (4.4) and (4.5) for the small x-behaviour of the scaling function is only consistent with a power ansatz (4.7) for the finite-size corrections of the initial values. Logarithmic corrections of the latter will induce logarithmic corrections in the small x-behaviour of the scaling functions.

Finally let us discuss equations (4.21) and (4.28) for the lowest excitations e_{10} and f_{10} from the ground state. The numerical results shown in Figures 2 and 3 tell us that the coefficients in the scaling functions for the higher excitations e_{03} and f_{03} are considerably smaller. If we neglect in equations (4.21) and (4.28) all higher excitations we find

$$e_{10} = 2\frac{b_{10}^2}{a_{10}^2}, \qquad (4.31)$$

and

$$e_{10} + f_{10} \simeq 0. \qquad (4.32)$$

A comparison of the slopes

$$e_{10} = 0.0196(8), \quad f_{10} = -0.0177(8), \qquad (4.33)$$

in Figures 2 and 3 demonstrates that equation (4.32) is indeed well satisfied. The numerical values of $a_{10} = 9.74(8)$, $b_{10} = 0.95(3)$, estimated from the data of figure 1, together with equation (4.4) yield a value $e_{10} = 0.019$. This is in agreement with equation (4.33) and might be seen as an indication that the neglect of higher excitations is justified.

5 The Heisenberg model in a dimerized field

The general features developed for the 1D spin-1/2 Heisenberg model in a staggered field can be applied to all Hamiltonians of the type

$$\mathbf{H}(\delta) \equiv \mathbf{H} + \delta\mathbf{H}_D \qquad (5.1)$$

where $\mathbf{H}$ is the unperturbed Hamiltonian (1.1) and $\mathbf{H}_D$ denotes a perturbation operator. As a further interesting example we want to discuss here the dimer operator

$$\mathbf{H}_D = 2\sum_{n=1}^{N}(-1)^n\mathbf{S}_n \cdot \mathbf{S}_{n+1}. \qquad (5.2)$$

Hamiltonians of type (5.1) with $\mathbf{H}_D$ as (5.2) have been discussed in the framework of (organic) spin-Peierls materials [25], where the interaction between linear antiferromagnetic chains and the three-dimensional phonon system causes a dimerization of the lattice [26–28]. In case of the more recently discovered inorganic spin-Peierls material CuGeO$_3$, reference [29], it turned out that in addition a next nearest neighbour coupling in the spin chain has to be considered [30]. We will not discuss the influence of such a term in this paper.

The evolution equation for the energy eigenvalues $E_n(\delta)$ and the transition amplitudes:

$$T_{mn}(N, \delta) = \langle\Psi_m(\delta)|\mathbf{H}_D|\Psi_n(\delta)\rangle \qquad (5.3)$$

are obtained from (2.4) and (2.5) by a simple substitution: $h \mapsto \delta$, $E_n(N, h) \mapsto E_n(N, \delta)$, and $T_{mn}(N, h) \mapsto T_{mn}(N, \delta)$. Note however, that the dimer operator (5.2) conserves the total spin in contrast to the staggered spin operator. Therefore, the excitations from the ground state are singlet states as well.

For the solution of the evolution equation we need the initial values for the excitation energies:

$$\lim_{N\to\infty} N\omega_{mn}(N, \delta = 0) = a_{mn}, \qquad (5.4)$$

and for the transition amplitudes:

$$T_{mn}(N, 0) = 0 \quad \text{for} \quad (-1)^{m+n} = 1, \qquad (5.5)$$
$$T_{mn}(N, 0) = b_{mn}N^\kappa \quad \text{for} \quad (-1)^{m+n} = -1. \qquad (5.6)$$

Equation (5.5) results from momentum conservation at $\delta = 0$ and the fact that the operator (5.2) changes the momentum by π. Equation (5.6) is an ansatz for the finite-size dependence of the transition amplitudes. Numerical data are shown for $T_{10}(N, 0)$ in Figure 5. They suggest an exponent $\kappa = 0.37(5)$, which deviates from the standard values $\kappa = 1/2$, predicted by conformal field theory [19,13]. The discrepancy is due to strong logarithmic corrections, which are disregarded in the fit (5.6). This leads to a shift of the exponent κ. We expect that the standard value $\kappa = 1/2$ will show up with increasing system size.

Next we study the finite-size scaling ansatz of the type (3.1) and (3.2):

$$\frac{\omega_{10}(N, \delta)}{\omega_{10}(N, 0)} = 1 + e_{10}(x) \qquad (5.7)$$

$$\frac{T_{10}(N, \delta)}{T_{10}(N, 0)} = 1 + f_{10}(x), \qquad (5.8)$$

for the lowest excitation energy $\omega_{10}(N, \delta)$ and transition amplitude $T_{10}(N, \delta)$. Numerical results are shown in Figure 6. Optimal scaling is achieved now with a scaling variable

$$x = N\delta^\epsilon, \quad \epsilon = 0.72(1), \qquad (5.9)$$

which is in good agreement with the value

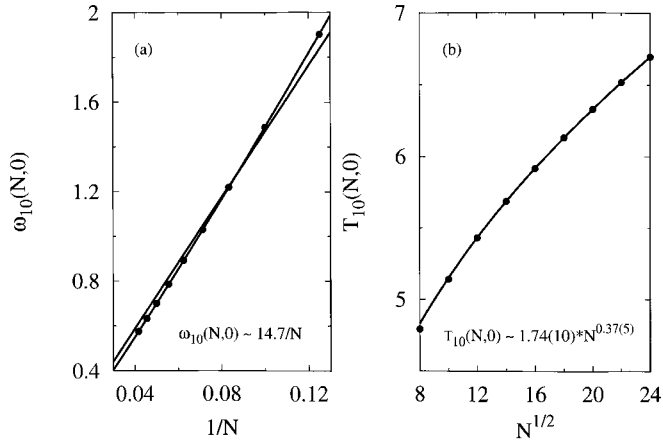$$\epsilon = (1 + \kappa)^{-1} \simeq 0.73(5), \qquad (5.10)$$

Fig. 5. Finite-size dependence of the ground state energy (a) and the corresponding transition amplitude (b) of Hamiltonian (5.1), for system sizes $N = 8, 10, \ldots, 24$ (•). The solid lines represent fits to the asymptotic behaviour (2.13) and (2.14).
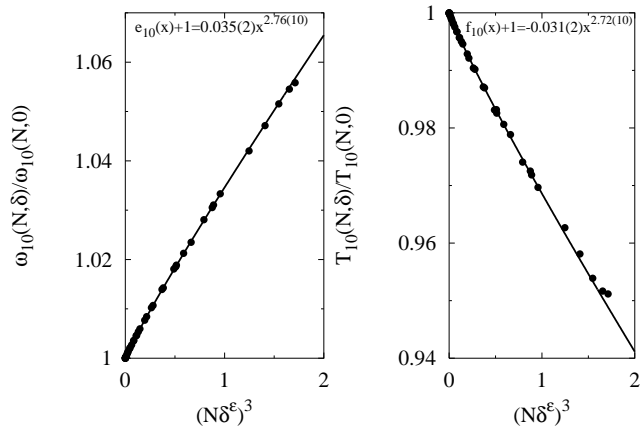

Fig. 6. The ratios (5.7) and (5.8) for $e_{10}(x)$ and $f_{10}(x)$ *versus* $(N\delta^\epsilon)^3$ with $\epsilon = 0.73$. The solid lines show the fits to the small x-behaviour.

which follows from the exponent $\kappa = 0.37(5)$ in the initial value shown in Figure 5. This value (5.10) is compatible with previous results extracted from a finite-size scaling analysis combined with renormalization group analysis [31–33].

The exponent ϕ in the small x-behaviour of the scaling functions $e_{10}(x)$ and $f_{10}(x)$ is in agreement with equation (5.10):

$$\phi = 2/\epsilon = 2.74(5). \tag{5.11}$$

The coefficients e_{10} and f_{10} in front:

$$e_{10} = 0.0346(8), \quad f_{10} = -0.0314(8), \tag{5.12}$$

obey the approximate relation (4.32). It is remarkable to note, that the relation (5.10) between the exponents ϵ and κ holds inspite of the fact that the *true* large N behaviour ($\kappa = 1/2$, $\epsilon = 2/3$) is not yet visible in the finite system

results. Affleck and Bonner [34] have discussed the implications of logarithmic corrections to critical exponents. They have comprised those corrections into effective scaling dimensions *i.e.* "critical exponents" and found $\epsilon = 0.78$ for chain length $N = 20$.

In the same way, as we have analysed the large x-behaviour of the scaling function (3.15) in a staggered field, we have extrapolated the gap in the presence of a dimerized field:

$$\Omega_{10}^\infty = 6.0(1). \tag{5.13}$$

6 Conclusions and perspectives

In this paper we have developed a general procedure to investigate the behaviour of antiferromagnetic Heisenberg chains, which are weakly perturbed by an external field. As examples we considered here a staggered field and a dimerized field, respectively.

The question of interest is: What happens with the excitation spectrum and transition amplitudes under the influence of the perturbation? The procedure used in this paper is based on the observation that excitation energies and transition amplitudes for the perturbation operator satisfy a system of differential equations (2.4) and (2.5), which describe the evolution in the strength h (or δ) of the external field. The initial conditions (2.10), (2.13) and (2.14) are completely fixed by the excitation spectrum and transition amplitudes of the unperturbed system ($h = 0, \delta = 0$). We have shown in Section 4 that a scaling ansatz ((4.1) and (4.2)) leads to a consistent solution of the evolution equations in the scaling limit (3.3). The exponents σ and ϵ in the scaling ansatz ((4.1), (4.2)) and the scaling variable Nh^ϵ are fixed by the finite-size behaviour of the initial conditions (2.10), (2.13) and (2.14).

We have also tested numerically the predictions of the scaling ansatz and found good agreement for the exponents as well as for the scaling functions for small values of the scaling variable. Therefore, the behaviour of the perturbed system in the scaling limit (3.3) is well understood.

To answer the question whether a gap opens in the presence of an external field (h fixed) in the thermodynamic limit ($N \to \infty$), demands the knowledge of the scaling functions (4.4) for large values of the scaling variable. In principle, this asymptotic behaviour follows from a solution of the differential equations (4.10), (4.11) and (4.12), (4.13) for the scaling functions using the initial conditions (4.4) and (4.5). In practice, it might be easier to study this limit numerically coming from finite system results. Our numerical data are consistent with a constant behaviour (3.15) of the gap scaling function.

The opening of a gap in a uniform field has been recently observed [35] in a neutron scattering experiment on copper benzoat $Cu(C_6D_5COO)_2 \cdot 3D_2O$. The existence of field dependent and field independent low energy modes at wave vectors $q = \pi(1 - 2M)$ and $q = \pi$, respectively, leads to the expectation, that the compound is adequately described by the Hamiltonian (1.2) in a uniform external

field $B\mathbf{S}_3(p = 0)$. This system is known to show up zero energy excitations at wave vectors $q = \pi(1 - 2M)$ and $q = \pi$ in the longitudinal and transverse structure factors, respectively [3,4,6].

The exponential fit to the temperature dependence of the specific heat data revealed, however, that there is a gap which opens with the field strength B as B^ϵ, $\epsilon \simeq 2/3$. This means of course, that the compound copper benzoat can not be described by (1.2) with $p = 0$. Oshikawa and Affleck [36] argued that the local g-tensor for the Cu-ions generates an effective staggered field of strength $h(= h(B) \ll B)$ perpendicular to the uniform field B. Therefore, one is lead to investigate the Hamiltonian:

$$\mathbf{H}(h) = \mathbf{H} + h\mathbf{S}_3(0) + B\mathbf{S}_1(\pi). \qquad (6.1)$$

The authors of reference [36] studied the model (6.1) for $B = 0$, which is just the case we investigated in this paper. They came to the same conclusion concerning the opening of the gap with h^ϵ, $\epsilon \simeq 2/3$, as we found here. The question remains, how the exponent ϵ changes if the uniform field B is switched on. Moreover, the gap might evolve in a different fashion for the field dependent and field independent soft modes $q = \pi(1 - 2M)$ and $q = \pi$. We will address these questions in a further publication [37].

References

1. M. Jimbo, T. Miwa, *Algebraic Analysis of Solvable Lattice Models*, *CBMS* (American Mathematical Society, Providence, 1995).
2. M. Karbach *et al.*, Phys. Rev. B 12510 (1997).
3. A. Fledderjohann *et al.*, Phys. Rev. B **54**, 7168 (1996).
4. G. Müller, H. Thomas, H. Beck, J.C. Bonner, Phys. Rev. B **24**, 1429 (1981).
5. M.D. Johnson, M. Fowler, Phys. Rev. B **34**, 1728 (1986).
6. M. Karbach, K.-H. Mütter, M. Schmidt, J. Phys.-Cond. **7**, 2829 (1995).
7. K. Lefmann, C. Rischel, Phys. Rev. B **54**, 6340 (1996).
8. J.P. Groen *et al.*, Phys. Rev. B **22**, 5369 (1980).
9. N. Ishimura, H. Shiba, Prog. Theor. Phys. **57**, 1862 (1977).
10. H. Schulz, Phys. Rev. Lett. **77**, 2790 (1996).
11. F.C. Alcaraz, M.N. Barber, M.T. Batchelor, Phys. Rev. Lett. **58**, 771 (1987).
12. F. Woynarovich, H.-P. Eckle, J. Phys. A: Math. Gen. **20**, L97 (1987).
13. F.C. Alcaraz, M.N. Barber, M.T. Batchelor, Ann. Phys. **182**, 280 (1988).
14. C. Hamer, M. Batchelor, M. Barber, J. Stat. Phys. **52**, 679 (1988).
15. K. Okamoto, K. Nomura, Phys. Lett. A **169**, 433 (1992).
16. K. Nomura, K. Okamoto, J. Phys. Soc. Jpn **62**, 1123 (1993).
17. K. Nomura, Phys. Rev. B **48**, 16814 (1993).
18. M. Karbach, K.-H. Mütter, J. Phys. A: Math. Gen. **28**, 4469 (1995).
19. M. den Nijs, Phys. Rev. B **23**, 6111 (1981).
20. P. Christe, M. Henkel, *Introduction to Conformal Invariance and its Applications to Critical Phenomena* (Springer-Verlag, Berlin Heidelberg, 1993).
21. V. Privman, M. Fisher, J. Stat. Phys. **33**, 385 (1983).
22. V. Privman, M. Fisher, Phys. Rev. B **30**, 32 (1984).
23. I. Affleck, D. Gepner, H.J. Schulz, T. Ziman, J. Phys. A: Math. Gen. **22**, 511 (1989).
24. R. Bulirsch, J. Stoer, Num. Math. **6**, 413 (1964).
25. I. Jacobs *et al.*, Phys. Rev. B **14**, 3036 (1976).
26. E. Pytte, Phys. Rev. B **10**, 4637 (1974).
27. L. Bulaevskii, A. Buzdin, D. Khomskii, Solid State Commun. **27**, 5 (1978).
28. M. Cross, D. Fisher, Phys. Rev. B **19**, 402 (1979).
29. M. Hase, I. Terasaki, K. Uchinokura, Phys. Rev. Lett. **70**, 3651 (1993).
30. K. Fabricius *et al.*, Phys. Rev. B **57**, 1102 (1998).
31. J.N. Fields, Phys. Rev. B **19**, 2637 (1979).
32. G. Spronken, B. Fourcade, Y. Lépine, Phys. Rev. B **33**, 1886 (1986).
33. H.W. Blöte, J.C. Bonner, Phys. Rev. B **36**, 2337 (1987).
34. I. Affleck, J. Bonner, Phys. Rev. B **42**, 954 (1990).
35. D. Dender *et al.*, Phys. Rev. Lett. **79**, 1750 (1997).
36. M. Oshikawa, I. Affleck, Phys. Rev. Lett. **79**, 2883 (1997).
37. A. Fledderjohann, K.-H. Mütter, M. Karbach, in preparation.